General Instantaneous Dynamic Phasor

Chun T. Rim, *Fellow, IEEE*, Syed Ahson Ali Shah, *Member, IEEE*, Hyo J. Park, Abhinandan Routray, Seog Y. Jeong, *Senior Member, IEEE*, and Youngjoo Chung, *Member, IEEE*

***Abstract*—Dynamic phasor has now been widely used in the fields of ac power and signal, such as power electronics, power systems engineering, and instrumentation. It is, however, broadly misunderstood by users that the dynamic phasor is valid for an averaged period of time. This misbelief stems from the definition of Fourier series coefficients for a variable where the time sliding integration is taken over a period to get its average. In this article, it is verified that the dynamic phasor is valid instantaneously for any time and that averaging over a period has nothing to do with the dynamics of phasor variables. An extended phasor transformation is newly proposed as a generalized instantaneous dynamic phasor. This instantly valid dynamic phasor is thoroughly verified by mathematics, simulation, and experiments. The instantaneous dynamic phasor is found to be valid for an arbitrary and even time-varying frequency, which is not necessarily the same as the source frequency. The transfer function of the phasor space system is found to be a frequency shift form of the original one of the real space system for the fixed frequency dynamic phasor.**

***Index Terms*—Dynamic phasor, generalized averaging, instantaneous dynamic phasor, Laplace transform, phasor transformation.**

I. Introduction

NOWADAYS ‘dynamic phasor’ is quite widely used in the fields of ac power and signal. It is a simple and powerful tool to deal with time-varying ac power and signals. More specifically, the envelope behavior of a sinusoidal waveform can be analyzed by the dynamic phasor. It would be useful for readers to briefly review the history of the dynamic phasor, highlighting a few monument papers.

The phasor concept was first adopted in electrical engineering in 1894 as of the static phasor form [1]. Although this was introduced in electrical engineering, it is applicable to all engineering and science areas, considering its mathematical formulation. Static phasor has been widely used for the steady-state analyses of ac power, communications, controls, and signal processing. There is so much literature that they are intentionally not provided here to highlight important references only.

So far as we have investigated, the dynamic phasor concept was first adopted in 1961, where the slowly varying phase and amplitude of a variable were examined [2]. Although not called “dynamic phasor” at that time, this concept evolved to “describing function technique” in 1968, where a dynamic phasor form solution is assumed for the analysis of transient oscillation [3]. The dynamic phasor concept presented in [2] and [3] is of a complex form, which neglects the real part operator that connects a real system and its corresponding complex system. There is no equivalent circuit available in the complex domain as well, which is inconvenient for engineers to use in theory. These would be parts of the reasons why there is not many literatures that use this early-stage dynamic phasor.

It was not until 1990 that the modern dynamic phasor became available as the name of “phasor transformation” [4]. A general dynamic phasor concept was proposed, which is instantly valid for any abrupt frequency and phase change of a variable. Dynamically equivalent circuits for *RLC* components, ac voltage/current sources, and ac switching converters in the complex domain are first provided. The real part operator is adopted to retrieve real variables from the complex variables. Thus, the method made it possible to obtain the dynamics of resonant converters with great ease.

A generalized averaging method was proposed in 1991 that applied the describing function technique to converter analysis [5]. This method adopts the Fourier series to represent periodic variables in converters. The time-varying Fourier coefficient is obtained by integrating for a window of length *T* slides over the actual waveform. In this way, the method had successfully expanded the theory of state-space averaging to ac converters. This paper referenced the literature [4] that obtained very similar results of “the time-varying phasor analysis.” Neither equivalent complex circuits nor real part operation were proposed in the generalized averaging method though.

After publications of the two papers, thousands of literatures have addressed dynamic phasor concept [6], [7], [8], [9], [10], [11], [12], [13], [14], [15], [16], [17], [18], [19], [20], which almost refer the two original dynamic phasor papers. Among them, “phasor dynamics” was applied to the analysis of converters in 1993 and 1997, where the convenient real part operation is used and only the fundamental component is considered, truncating all the other harmonics [6], [7]. The exact keyword “dynamic

Received 10 September 2024; revised 15 January 2025 and 22 May 2025; accepted 1 July 2025. Date of publication 8 July 2025; date of current version 27 August 2025. This work was supported by the National Research Foundation of Korea (NRF) grant funded by the Korea government (MSIT) under Grant RS-2023-00302281 and Grant RS-2024-00427153. Recommended for publication by Associate Editor L. Corradini. *(Corresponding author: Chun T. Rim.)*

Chun T. Rim, Syed Ahson Ali Shah, Hyo J. Park, and Youngjoo Chung are with the Department of Electrical Engineering and Computer Science, Gwangju Institute of Science and Technology, Gwangju 61005, South Korea (e-mail: ctrim@gist.ac.kr; sahsonas@gist.ac.kr; 20215099@gm.gist.ac.kr; ychung@gist.ac.kr).

Abhinandan Routray is with the Department of Electrical and Electronics Engineering, Manipal Institute of Technology, Manipal Academy of Higher Education, Manipal 576104, India (e-mail: abhinandan.routray@manipal.edu).

Seog Y. Jeong is with Samsung Electronics Company, Ltd., Seoul 06765, South Korea (e-mail: seogy.jeong@samsung.com).

Color versions of one or more figures in this article are available at https://doi.org/10.1109/TPEL.2025.3587094.

Digital Object Identifier 10.1109/TPEL.2025.3587094

phasor" was first used in 1999, whose concept is the same as provided in the previous papers [6], [7], but the name had been changed [8]. So, it is not true that "dynamic phasor was first introduced in 2007" [11], which is 17 years after the first modern dynamic phasor introduction and 8 years after the first use of the same name.

Active societies and journals that use the dynamic phasor concept are found to be power electronics, power systems, instrumentation and measurement, etc. Some of them are reviewing and referencing publications of other areas; however, many of them still exchange information within their own areas and do not even use the dynamic phasor method, although highly needed. The merits and limitations of the dynamic phasor are often not clearly addressed.

One of the widely misunderstood facts is that a dynamic phasor is valid only when the variable is averaged over a period *T*. This misbelief stems from the definition of Fourier series coefficients for a variable where the time sliding integration is taken over a period to get its average. In this article, it is verified that the dynamic phasor is valid instantaneously for any time and that averaging over a period has nothing to do with the dynamics of phasor variables. This instantly valid dynamic phasor is generally verified by mathematics, simulation, and experiments throughout this article.

II. Theory on Instantaneous Dynamic Phasor

Since most dynamic phasor papers originate from the two original dynamic phasor papers, the "phasor transformation [4]" and "generalized averaging method [5]" are retrieved, interpreted, and compared with each other to make the concept of "instantaneous dynamic phasor" clear. An extended phasor transformation as a generalized instantaneous dynamic phasor is introduced here. As this is not a review article, new aspects of the two dynamic phasor techniques, which are not well known, are to be highlighted.

A. Proposed Extended Phasor Transformation

The representation of the general unified phasor transformation [15] is retrieved here in the standard form, which is the non-rms value of a variable $x(t)$, as follows:

$$x(t) = \mathrm{Re}\left\{\frac{1}{\sqrt{m}}\mathbf{x}(t)\, e^{j\theta(t)}\right\} \text{ for } -\infty < t < \infty \quad (1)$$

where $\mathbf{x}(t)$ is the corresponding complex variable, $\theta(t)$ is an arbitrary nonzero phase angle, and *m* is the number of poly phases, i.e., $m = 1$ for single phase and $m = 3$ for three phase. Note that originally $\theta(t) = \omega_s t$ [4] and it is here extended to an arbitrary phase angle. This phasor transformation of (1) had unified the three-phase case to the single-phase transformation [4] and generalized to an arbitrary frequency and phase case in this article. Because this aspect is important for the proposed instantaneous dynamic phasor, it is explained in detail.

It should be noted from (1) that $\theta(t)$is not necessarily linear to time *t* but nonlinear to *t*; so, it could be a square wave or frequency modulation (FM) signal as follows:

$$\theta(t) = \omega_0 t + \alpha \sin\omega_1 t \quad (2)$$

where ω_0, ω_1, and α are arbitrary constant values. Moreover, $\theta(t)$ is not necessarily a continuous waveform but a discontinuous waveform, such as a step function and a delta function. So, $e^{j\theta(t)}$ is not necessarily a periodic function. Under these severely changing extreme conditions of $\theta(t)$, (1) is still valid for all the time. This means that $\mathbf{x}(t)$ always exist for any $x(t)$ and vice versa, which shall be more rigorously verified in the following. For practical utility, $\theta(t)$should be chosen to simplify the resulting system equations, reflect the dominant frequency content of the signal, and ensure that the corresponding phasor $\mathbf{x}(t)$ varies as slowly as possible over time.

It is straightforward that $x(t)$ exists for any $\mathbf{x}(t)$ from (1). The reverse, however, is not true. In general, a complex variable $\mathbf{x}(t)$ is composed of its magnitude and phase terms as $|\mathbf{x}(t)|e^{j\angle\mathbf{x}(t)}$; therefore, it can be represented as an example, for a given $x(t)$, as follows:

$$\mathbf{x}(t) = \sqrt{m}x(t)\, e^{-j\theta(t)}. \quad (3)$$

Then, applying (3) to (1) becomes

$$x(t) = \mathrm{Re}\left\{\frac{1}{\sqrt{m}}\sqrt{m}x(t)\, e^{-j\theta(t)}e^{j\theta(t)}\right\} = x(t). \quad (4)$$

For an example of an extreme case, (3) can be found for a unit step function $u(t)$ of $x(t)$ and $\theta(t)$ of (2) as follows:

$$\mathbf{x}(t) = \sqrt{m}u(t)\, e^{-j(\omega_0 t + \alpha \sin\omega_1 t)}. \quad (5)$$

As identified from (5), $\mathbf{x}(t)$ is neither a stationary phasor nor a slowly varying continuous variable in time.

The time derivative of (1) becomes as follows:

$$\dot{x}(t) = \mathrm{Re}\left[\frac{1}{\sqrt{m}}\left\{\dot{\mathbf{x}}(t) + j\,\dot{\theta}(t)\,\mathbf{x}(t)\right\}e^{j\theta(t)}\right] \quad (6)$$

where the arbitrary phase $\theta(t)$ assumed to be differentiable.

Note that the phasor transformation of (1) and (3) has nothing to do with the Fourier series; therefore, no averaging of $x(t)$over a period of *T* is needed.

As identified from (4), $x(t)$ and $\mathbf{x}(t)$ are in 1-to-1 mapping relationship at all times so far as (3) is met. So, $\mathbf{x}(t)$ is the instantaneously valid dynamic phasor of $x(t)$ for arbitrary $\theta(t)$.

As shown in Fig. 1, applying the dynamic phasor of (1) to *RLC* circuits in real space results in complex *RLC* circuits with imaginary impedance in phasor space.

Let us consider the linear time-invariant inductor case first, assuming $m = 1$ from now on for simplicity, as follows:

$$L\dot{i}_L(t) = v_L(t) \quad (7a)$$

$$\rightarrow L\dot{i}_L(t) = L\mathrm{Re}\left[\left\{\dot{\mathbf{i}}_\mathrm{L}(\mathrm{t}) + \mathrm{j}\,\dot{\theta}(\mathrm{t})\,\mathbf{i}_\mathrm{L}(\mathrm{t})\right\}\mathrm{e}^{\mathrm{j}\theta(\mathrm{t})}\right]$$

$$= \mathrm{Re}\left\{\mathbf{v}_\mathrm{L}(\mathrm{t})\,\mathrm{e}^{\mathrm{j}\theta(\mathrm{t})}\right\} \quad (7b)$$

$$L\dot{\mathbf{i}}_L(t) + j\dot{\theta}(t)\,L\mathbf{i}_L(t) \equiv L\dot{\mathbf{i}}_L\overset{\leftrightarrow}{(t)} + jX_L(t)\,\mathbf{i}_L(t) = \mathbf{v}_L(t). \quad (7c)$$

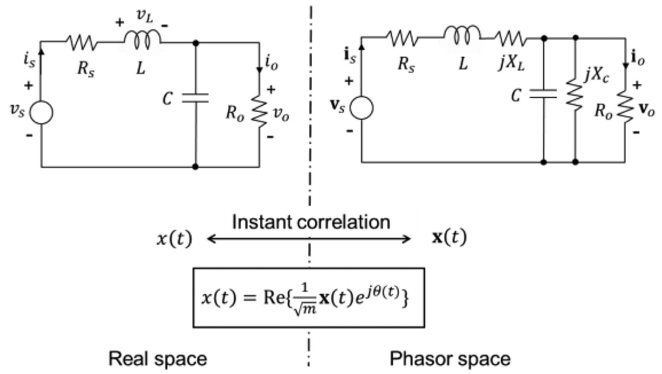

Fig. 1. Proposed instantaneous dynamic phasor in time domain.

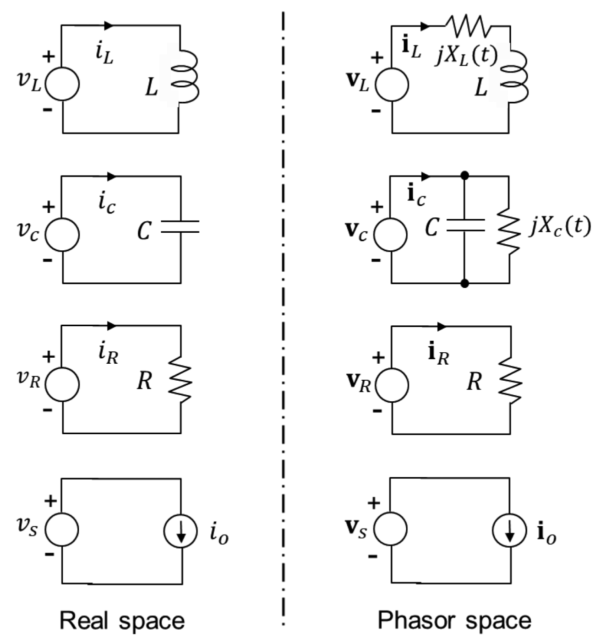

Fig. 2. Instantaneous dynamic phasor of *LCR* circuits and voltage or current sources for arbitrary phase $\theta(t)$.

The equivalence of (7b) and (7c) is proved in the literature [15] for any time-varying $\theta(t)$, which is not a constant value. The phasor transformation for *RLC* components including inductor is described in more detail in [4], Sec. II-B. Note from (7b) that the time-varying reactance becomes time-invariant only when the phase $\theta(t)$ is linear w.r.t. time *t*, i.e., $\theta(t) = \omega t$ as follows:

$$X_L\ (t) = \dot{\theta}\ (t)\, L\ =\ \omega L \tag{8}$$

which is the well-known reactance of an ac inductor; however, this reactance is valid not only for the static case but also for the dynamic case. The results for (7) are drawn in the circuits of Fig. 2, removing "(*t*)" term for simplicity, except for the time-varying reactance.

In a very similar fashion, the instantaneous dynamic phasor for a linear time-invariant capacitor becomes as follows:

$$C\dot{v}_c\,(t) = i_c\,(t) \tag{9a}$$

$$C\dot{\mathbf{v}}_c\,(t) + j\dot{\theta}\,(t)\,C\mathbf{v}_c\,(t) \overset{\leftrightarrow}{\equiv} C\dot{\mathbf{v}}_c\,(t) + \frac{\mathbf{v}_c\,(t)}{jX_c\,(t)} = \mathbf{i}_c\,(t) \tag{9b}$$

$$X_c\,(t) \equiv -1/\left\{\dot{\theta}\,(t)\,C\right\} = -1/\,(\omega C)\ for\ \theta\,(t) = \omega t. \tag{9c}$$

The instantaneous dynamic phasor for a linear time-invariant resistance also becomes as follows:

$$Ri_R\,(t) = v_R\,(t) \leftrightarrow R\mathbf{i}_R\,(t) = \mathbf{v}_R\,(t)\,. \tag{10}$$

The instantaneous dynamic phasor for a voltage and current source is defined from (1), given as follows:

$$v_s\ (t) = \mathrm{Re}\left\{\mathbf{v}_s\,(t)\,e^{j\theta(t)}\right\} = \mathrm{Re}\left\{\mathbf{v}_s(t)\,e^{j\omega t}\right\}\ \text{for}\,\theta\ (t) = \omega t \tag{11a}$$

$$i_o\ (t) = \mathrm{Re}\ \left\{\mathbf{i}_o\,(t)\,e^{j\theta(t)}\right\} = \mathrm{Re}\ \left\{\mathbf{i}_o\,(t)\,e^{j\omega t}\right\}\ \text{for}\ \theta\,(t) = \omega t. \tag{11b}$$

Note from (11) that $\mathbf{v}_s(t)$ and $\mathbf{i}_o(t)$ would become slowly varying envelopes of $v_s(t)$and $i_o(t)$, respectively, if $v_s(t)$and $i_o(t)$ are sinusoidal waveforms of ω. However, this is not the mandatory condition for the instantaneous dynamic phasor of (1). So, the dynamic phasor so far discussed above is valid for arbitrary source and output frequencies which could be different from ω, i.e., $\omega \neq \omega_s \neq \omega_o$.

As a summary, it can be said that the dynamic phasor, as shown in Figs. 1 and 2, instantly relate the real space with the phasor space for arbitrary time-varying phase or arbitrary nonzero frequency. Of course, a practically useful dynamic phasor is only obtained for $\omega = \omega_s\ = \omega_o$.

B. Reinterpretation of the Generalized Averaging

The original generalized averaging method [5] is retrieved here because there is no change in the principle of the techniques despite the change of names to dynamic phasor now.

The waveform *x*(*t*) is expanded on the interval (*t* - *T*, *t*] in a Fourier series representation of the form

$$x\,(t - T + s) = \sum_{k=-\infty}^{\infty} \langle x\rangle_k\,(t)\,e^{jk\omega_s(t-T+s)} \tag{12}$$

where the sum is over all integers *k* and $\omega_s = 2\,\pi\,/T$, $s \in (0, T]$, and $\langle x\rangle_k(t)$ are complex Fourier coefficients as follows:

$$\langle x\rangle_k\,(t) = \frac{1}{T}\int_0^T x\,(t - T + s)\,e^{-jk\omega_s(t-T+s)}ds. \tag{13}$$

Since (13) is an average value over the past time of *T*, the generalized averaging model needs all the information on $x(t - T + s)$ for $s\ \in\ (0,\ T]$. In other words, we should wait for a period of time *T* to get the dynamic phasor information.

The time derivative of the *k*th Fourier coefficient becomes

$$\frac{d}{dt}\langle x\rangle_k\,(t) = \left\langle \frac{d}{dt}x \right\rangle_k (t) - jk\omega_s\langle x\rangle_k\,(t)\,. \tag{14}$$

It is interesting that (14) is also valid for a partial averaging case on the interval $s \in (t - \Delta T, t]$, where $0 < \Delta T < T$ as follows:

$$\langle x \rangle_k (t) = \frac{1}{\Delta T} \int_0^{\Delta T} x(t - \Delta T + s) e^{-jk\omega_s (t - \Delta T + s)} ds \quad (15)$$

which is no longer the Fourier coefficient; so, the Fourier series of (12) is not valid for (15). If this partial averaging of (15) is effective, we do not have to wait for a period of time T to get the dynamic phasor information. Note that (14) is also valid for any ΔT, which is arbitrarily large, i.e., $T \leq \Delta T$.

In practice, reasonably enough time is requisite for achieving reliable dynamic phasor information, which could be eventually multiples of T considering periodic switching harmonics. The calculation time T_c for the dynamic phasor, however, it is not necessarily governed by T as identified from the literature, for example, [16] and [17]. Either $T_c \leq T$ or $T_c > T$ is possible according to the signal processing algorithm. Although $T_c = T$ is often preferred due to periodic characteristics of switching converters, it is inherently nothing to do with the validation of (14).

As (14) is applied to an *RLC* circuit with voltage and current sources in real space, an equivalent circuit in the phasor space can be obtained. The example for an inductor is as follows:

$$L\frac{d}{dt}\langle i \rangle_k (t) = \left\langle L\frac{d}{dt} i \right\rangle_k (t) - jk\omega_s L \langle i \rangle_k (t)$$
$$= \langle v \rangle_k (t) - jk\omega_s L \langle i \rangle_k \quad (16a)$$

$$\rightarrow \; L\frac{d}{dt}\langle i \rangle_k (t) + jk\omega_s L \langle i \rangle_k = \langle v \rangle_k (t). \quad (16b)$$

Note that (16b) is the same form of (7c) and that the application of the generalized averaging model to other circuits, such as C and R, also has similar forms of (9) and (10) if only $\dot{\theta}(t) = \omega = k\omega_s$.

It should be remarked that even though we can get the dynamic phasor information with (15), there is no way to relate its corresponding (14) with (12) at the moment. In other words, it has been verified that extending the generalized averaging to the partial averaging case is not possible.

C. *Comparison of Dynamic Phasors*

There are a few differences among the dynamic phasor models: the phasor transformation, the generalized averaging, and the proposed extended dynamic phasor.

As summarized in Table I, one of them is its validity in the time domain. Inherently, the phasor transformation and its extended version proposed here are valid for the instantaneous time domain, but the generalized averaging is not instantaneously valid for.

Different from the single frequency of the phasor transformation, however, multiple switching harmonics can be examined by the generalized averaging model. The extended phasor transformation, however, enables us to use an arbitrary phase angle, which embraces nonperiodic switching cases and multiple harmonics.

TABLE I
COMPARISON OF DYNAMIC PHASOR MODELS

Comparison Issues	Original Phasor Transformation [4]	The Generalized Averaging [5]	Proposed Extended Phasor Transformation
Validity	Instantaneously	Averaged only	Instantaneously
Frequency	Single ($\omega = \omega_s$)	Multiple ($\omega = k\omega_s$)	Arbitrary $\dot{\theta}(t)$
Phase	-	-	Arbitrary $\theta(t)$
Periodicity	Must be periodic	Must be periodic	Need not periodic
Eq. circuit	Available	Not available	Available
Fourier series	Not needed	Requisite	Not needed
Switching converter	Auto transformer	Describing function	Auto transformer
LC resonant circuit	Reduced order possible	No reduced order	Reduced order possible

The phasor transformation and its extended version have several merits over the generalized averaging. Equivalent circuits in the phasor space are always available, including switching converters, which are found to be time-invariant auto-transformers. A serial or parallel *LC* resonant circuit of the second-order system can be degenerated to the first order for the tuned case and the zeroth order system for the mistuned case.

III. LAPLACED DYNAMIC PHASOR

In the ac power analyses, Laplace domain equivalent circuits are quite useful and highly needed for the system design. For simplicity, the Laplace transformation is applied to the dynamic phasor at a fixed frequency with time-varying amplitude as follows:

$$x(t) = \mathrm{Re}\left\{ \mathbf{x}(t) e^{j\omega_s t} \right\}. \quad (17)$$

The term "Laplaced" is adopted in this article as the abbreviation of "Laplace transform of," which is a quite widely used word in modeling.

A. *Laplaced* LCR *Circuits of Dynamic Phasor*

The dynamic phasor equation for a linear time-invariant inductor of (7) under the condition of (8) is examined as follows:

$$L\dot{\mathbf{i}}_L(t) + j\omega L \mathbf{i}_L(t) = \mathbf{v}_L(t). \quad (18)$$

Note that the Laplace transformation for the general instantaneous dynamic phasor of (7) does not give us of simple and conventional linear form of results. Since (18) is of linear time-invariant form, the Laplace transform can be applied to this equation, which is as follows:

$$(s + j\omega) L I_L(s) = V_L(s) \leftrightarrow I_L(s) = \frac{V_L(s)}{(s + j\omega) L}. \quad (19)$$

Bold characters are not used for the Laplace variables because it is a convention. In a similar fashion, the Laplace transformed capacitor and resistor of (9) and (10) under (8) become

$$(s + j\omega) C V_c(s) = I_c(s) \leftrightarrow V_c(s) = \frac{I_c(s)}{(s + j\omega) C}. \quad (20a)$$

$$R I_R(s) = V_R(s). \quad (20b)$$

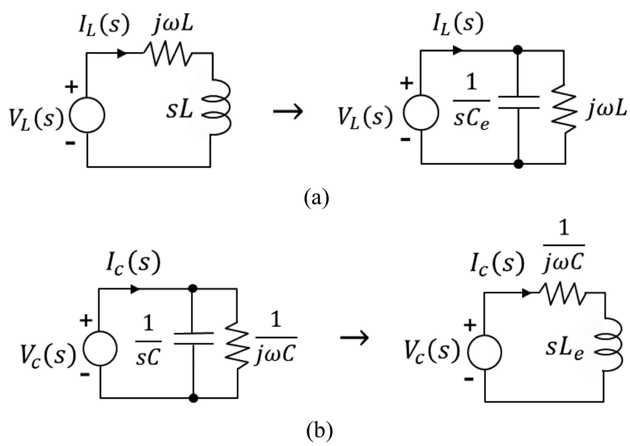

Fig. 3. Approximated equivalent circuits (right side) for (a) Laplaced inductor and (b) capacitor in the phasor space.

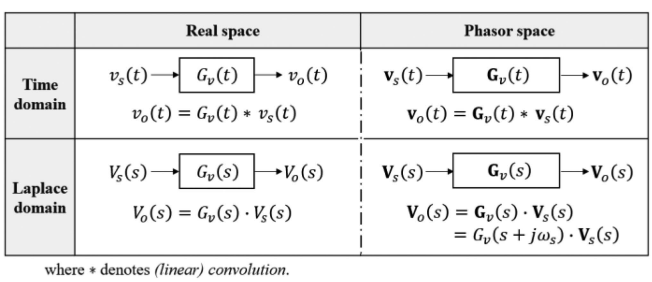

Fig. 4. System gains in the real space (left) and phasor space (right), where the frequency shift is found.

It is noteworthy that (19) and (20a) can be approximated for slow dynamics, respectively, as follows: <?TeX

$$I_L\ (s) = \frac{V_L\,(s)}{j\omega L\left(1+\frac{s}{j\omega}\right)} \cong \frac{V_L\,(s)}{j\omega L}\left(1-\frac{s}{j\omega}\right)$$
$$= V_L\ (s)\left(\frac{1}{j\omega L}+\frac{s}{\omega^2 L}\right)$$
$$\equiv \frac{V_L\,(s)}{j\omega L} + sC_e V_L\,(s). \qquad \because\ C_e = \frac{1}{\omega^2 L} \tag{21a}$$

$$V_c\ (s) = \frac{I_c\,(s)}{j\omega C\,(1+s/j\omega)} \cong \frac{I_c\,(s)}{j\omega C}\left(1-\frac{s}{j\omega}\right)$$
$$= I_c\ (s)\left(\frac{1}{j\omega C}+\frac{s}{\omega^2 C}\right)$$
$$\equiv \frac{I_c\,(s)}{j\omega C} + sL_e I_c\,(s) \qquad \because\ L_e = \frac{1}{\omega^2 C} \tag{21b}$$
$$\text{for } |\,s\,| \ll \omega. \tag{21c}$$

From (21a) and (21b), it is identified that the Laplace transformed inductor (capacitor) in the phasor domain can be approximated to an imaginary resistor in parallel (series) with an equivalent capacitor (inductor), as shown in Fig. 3 . Interestingly, the approximated equivalent circuit for an inductor resembles the capacitor circuit and vice versa. Note that this equivalence is valid only for the condition of (21c), which is found for specific *LC* resonant tank circuits only [4], but is now proved to be valid for any ac circuits in general.

B. Laplaced Sources of Dynamic Phasor

In case the source voltage or current of a linear time-invariant ac power system is sinusoid at a fixed frequency and phase with time-varying amplitude, the Laplace transform can be applied to the system. For example, the source voltage $v_s(t)$in Fig. 1 can be represented as the product of an envelope function $v_e(t)$of real value and a sinusoid with a fixed frequency and phase ϕ_s as follows:

$$v_s\ (t)\ \equiv v_e\ (t)\cos(\omega_s t+\phi_s)\ = \mathrm{Re}\left\{\mathrm{v_e}\ (\mathrm{t})\ \mathrm{e}^{\mathrm{j}\omega_s \mathrm{t}+\mathrm{j}\phi_s}\right\}. \tag{22}$$

The dynamic phasor of (22) is found for $m = 1$, for simplicity without the loss of generality, and the fixed frequency of ω_s from (1) as follows:

$$v_s\ (t)\ = \mathrm{Re}\left\{\mathbf{v}_s\ (t)\ e^{j\omega_s t}\right\}. \tag{23}$$

Comparing (23) with (22), the voltage source of the dynamic phasor is deduced as follows:

$$\mathbf{v}_s\ (t) = v_e\ (t)\, e^{j\phi_s}. \tag{24}$$

The transfer function of the real space circuit at the left side of Fig. 1 is canonically obtained as follows:

$$G_v\ (s) \equiv \frac{V_o\ (s)}{V_s\ (s)} = \frac{R_o}{(R_s+sL)\,(1+sCR_o)+R_o}. \tag{25}$$

Applying the Laplace transform to (22) results in the following:

$$V_s\ \ (s)\ = \mathcal{L}\left\{v_e\ (t)\ \frac{e^{j\omega_s t+j\phi_s}+e^{-j\omega_s t-j\phi_s}}{2}\right\}$$
$$= \frac{V_e\,(s-j\omega_s)\,e^{j\phi_s}+V_e\,(s+j\omega_s)\,e^{-j\phi_s}}{2}$$
$$= \frac{\mathbf{V}_s\,(s-j\omega_s)+\mathbf{V}_s^*\,(s+j\omega_s)}{2}. \tag{26}$$

Because (23) is the same form of the dynamic phasor of (17), any variables $x(t)$and $\mathbf{x}(t)$ in the time domain is Laplace transformed as follows:

$$X\ \ (s) = \frac{\boldsymbol{X}\,(s-j\omega_s)+\boldsymbol{X}^*\,(s+j\omega_s)}{2}. \tag{27}$$

Note from (26) that the Laplace transform of (24) of the following is used, where the bold character is used to distinguish the Laplaced phasor space variable from the real space variable.

$$\mathbf{V}_s\ \ (s) = V_e\ \ (s)\, e^{j\phi_s}. \tag{28}$$

Then, the Laplaced output voltage in real space can be determined from (25) and (26) as the linear sum of the well-known positive and negative sequence phasors as follows:

$$V_o\ \ (s)\ = G_v\ \ (s)\, V_s\ \ (s)$$
$$= G_v\ \ (s)\ \frac{\mathbf{V}_s\,(s-j\omega_s)+\mathbf{V}_s^*\,(s+j\omega_s)}{2}. \tag{29}$$

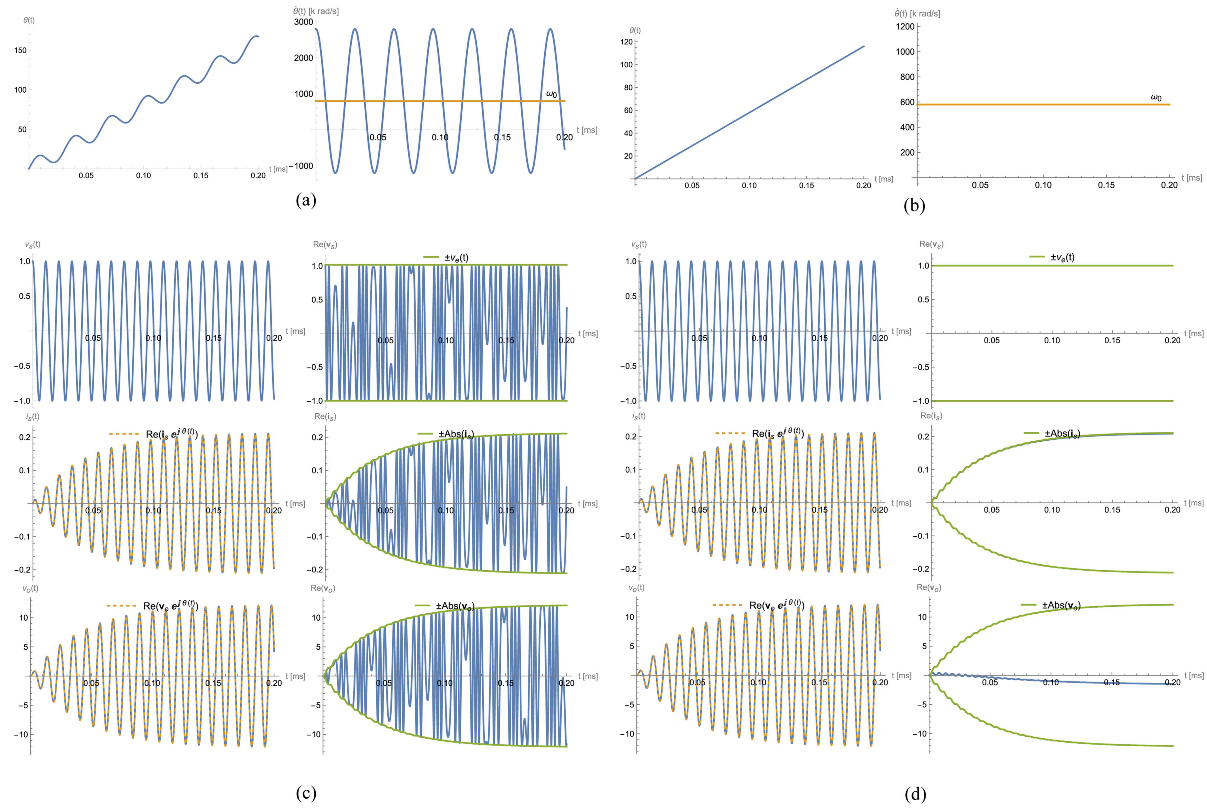

Fig. 5. Simulation of the proposed instantaneous dynamic phasor (left) and generalized averaging (right) for the left and right circuits of Fig. 1 by Mathematica at ω_s= 580 k rad/s. (a) $\theta(t) = \omega_0 t + \alpha \sin\omega_1 t$ (left), and its angular frequency (right). (b) $\boldsymbol{\theta}(t) = \boldsymbol{\omega}_0 t$ (left), and its angular frequency (right). (c) $v_s(t)$, $i_s(t)$, and $v_o(t)$ in real space compared with dynamic phasor (dotted yellow) (left), and $\mathbf{v}_s$, $\mathbf{i}_s$, and $\mathbf{v}_o$in phasor space (right). (d) $\boldsymbol{v_s}(t)$, $\boldsymbol{i_s}(t)$, and $\boldsymbol{v_o}(t)$ in real space compared with dynamic phasor (dotted yellow) (left), and $\mathbf{v_s}$, $\mathbf{i_s}$, $\mathbf{v_o}$ in phasor space (right).

Dynamic phasor and its Laplace transform of the output voltage $v_o(t)$ are found from (17) assuming zero initial conditions of the system as follows:

$$v_o(t) = \text{Re}\left\{\mathbf{v}_o(t)\ e^{j\omega_s t}\right\} \tag{30a}$$

$$\therefore\ V_o(s) = \mathcal{L}\left[\text{Re}\left\{\mathbf{v}_o(t)\ e^{j\omega_s t}\right\}\right] = \text{Re}\left[\mathcal{L}\left\{\mathbf{v}_o(t)\ e^{j\omega_s t}\right\}\right]$$
$$= \text{Re}\ \left[\mathbf{V}_o(s - j\omega_s)\right] = \frac{\mathbf{V}_o(s - j\omega_s) + \mathbf{V}_o^*(s + j\omega_s)}{2}. \tag{30b}$$

Applying (30b) to (29) results in the following equation.

$$\mathbf{V}_o(s - j\omega_s) + \mathbf{V}_o^*\ (s + j\omega_s)$$
$$= G_v(s)\left\{\mathbf{V}_s(s - j\omega_s) + \mathbf{V}_s^*(s + j\omega_s)\right\} \tag{31}$$

which holds for any s: therefore, replacing s with $s + j\omega_s$ results in the following frequency-shifted form:

$$\mathbf{V}_o(s) + \mathbf{V}_o^*\ (s + 2j\omega_s)$$
$$= G_v(s + j\omega_s)\left\{\mathbf{V}_s(s) + \mathbf{V}_s^*(s + 2j\omega_s)\right\} \tag{32}$$

Equation (32) can be decomposed into the following two equations:

$$\mathbf{V}_o\ (s) = G_v\ (s + j\omega_s)\,\mathbf{V}_s(s) \tag{33a}$$

$$\mathbf{V}_o^*\ (s + 2j\omega_s) = G_v\ (s + j\omega_s)\,\mathbf{V}_s^*(s + 2j\omega_s) \tag{33b}$$

Equation (33b) can be further simplified by replacing s with $s - 2j\omega_s$ as follows:

$$\mathbf{V}_o^*\ (s) = G_v\ (s - j\omega_s)\,\mathbf{V}_s^*(s). \tag{33c}$$

Note that (33c) is just the complex conjugate of (33a). Therefore, (33b) and (33c) are simply a degenerated form of (33a).

As shown in Fig. 4, the transfer function of the phasor space system is found to be a frequency shift form of the original one of the real space as follows:

$$\mathbf{G}_v(s) \equiv \frac{\mathbf{V}_o(s)}{\mathbf{V}_s(s)} = G_v\ (s + j\omega_s). \tag{34}$$

For the proposed example circuit of (25), the system gain in the phasor space of (34) is calculated as follows:

$$\mathbf{G}_v\ (s) = \frac{R_o}{\left\{R_s + (s + j\omega_s)\,L\right\}\left\{1 + (s + j\omega_s)\,CR_o\right\} + R_o}. \tag{35}$$

Note that (35) is exactly the same as the circuit transfer function of the right part in Fig. 1. As shown in Fig. 4, the envelope behavior, instead of the real-time sinusoid waveform, is directly obtained from the system gain of the phasor space.

IV. Simulation for Instantaneous Dynamic Phasor

The proposed extended phasor transformation, as the instantaneous dynamic phasor, is verified by simulation here. For

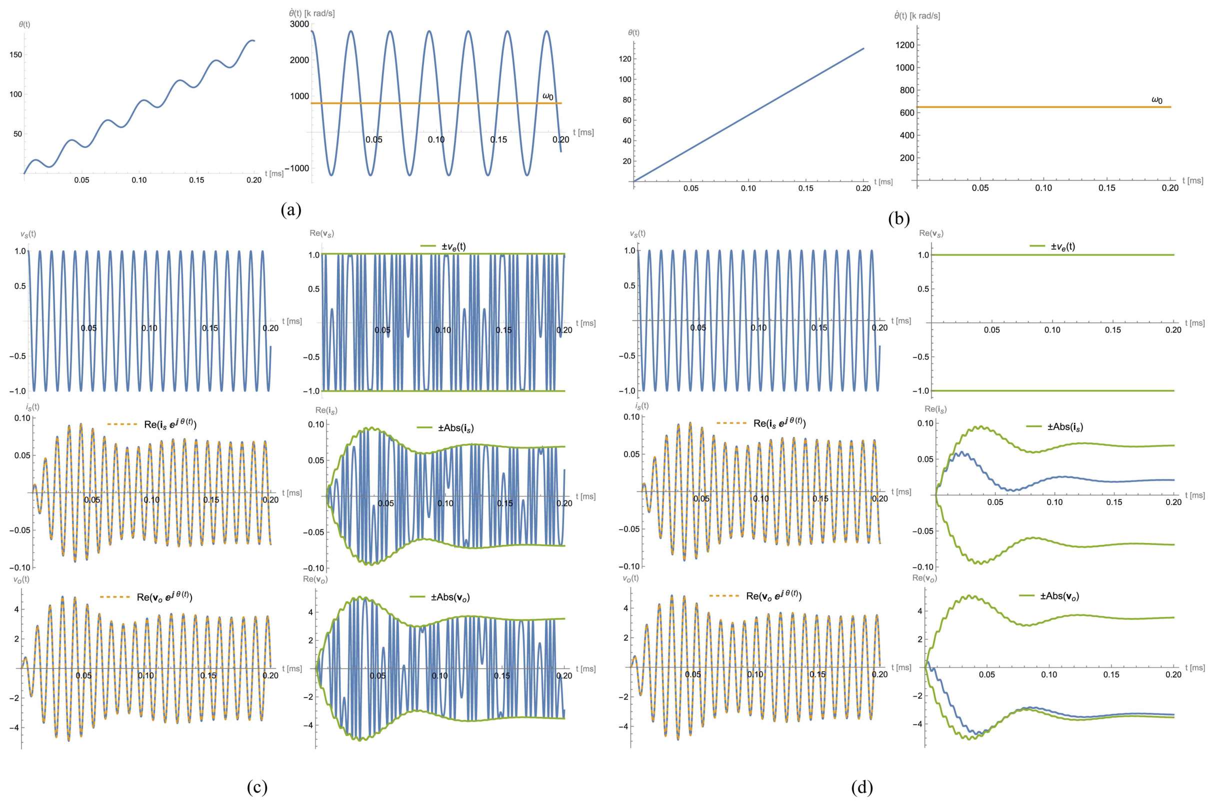

Fig. 6. Simulation of the proposed instantaneous dynamic phasor (left) and generalized averaging (right) for the left and right circuits of Fig. 1 by Mathematica at ω_s= 650 krad/s. (a) $\theta(t) = \omega_0 t + \alpha \sin\omega_1 t$ (left), and its angular frequency (right). (b) $\boldsymbol{\theta}(t) = \boldsymbol{\omega}_0 t$ (left), and its angular frequency (right). (c) $v_s(t)$, $i_s(t)$, and $v_o(t)$ in real space compared with the dynamic phasor (dotted yellow) (left), and $\mathbf{v}_s$, $\mathbf{i}_s$, and $\mathbf{v}_o$in phasor space (right). (d) $\boldsymbol{v_s}(t)$, $\boldsymbol{i_s}(t)$, and $\boldsymbol{v_o}(t)$ in real space compared with the dynamic phasor (dotted yellow) (left), and $\mathbf{v_s}$, $\mathbf{i_s}$, and $\mathbf{v_o}$in phasor space (right).

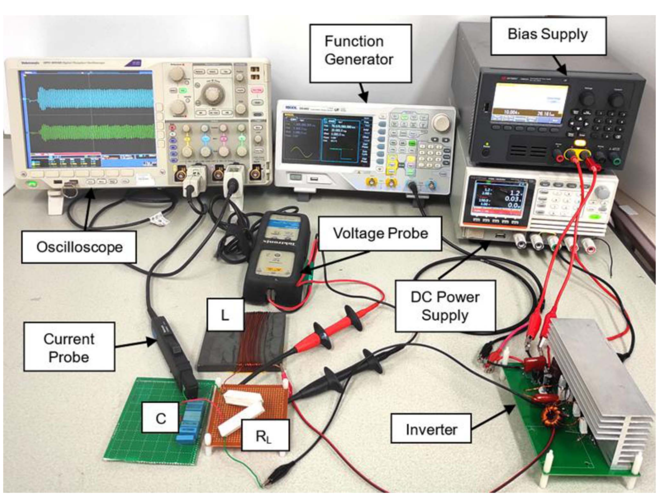

Fig. 7. Experiment kit for the circuit of Fig. 1.

simplicity and showing practical feasibility in a real worthy application in the power electronic field, we have implemented our proposed theory on an *RLC* circuit. The extended phasor transformation of (1) is applied to an example circuit of an *RLC* resonant circuit of Fig. 1. The phasor is assumed to be (2). Then, the time-varying reactance for *L* and *C* can be determined from (8) and (9c) as follows:

$$X_L(t) \equiv \dot{\theta}(t) L = (\omega_0 + \alpha\omega_1 \cos\omega_1 t) L \tag{36a}$$

$$X_c(t) \equiv -\frac{1}{\left\{\dot{\theta}(t) C\right\}} = -\frac{1}{\{(\omega_0 + \alpha\omega_1 \cos\omega_1 t) C\}}. \tag{36b}$$

The *RLC* circuit in the phasor space of Fig. 1 is linear time-varying and can be represented as a state equation as follows:

$$L\,\dot{\mathbf{i}}_s = \mathbf{v}_s - \{R_s + jX_L(t)\}\,\mathbf{i}_s - \mathbf{v}_o \tag{37a}$$

$$C\,\dot{\mathbf{v}}_o = \mathbf{i}_s - \mathbf{v}_o/R_o - \mathbf{v}_o/jX_c(t). \tag{37b}$$

Given the source voltage of (22), its dynamic phasor for the FM signal of (2) becomes the following:

$$v_s(t) = \mathrm{Re}\left\{ v_e(t)\, e^{j\omega_s t + j\phi_s}\right\} \equiv \mathrm{Re}\left\{\mathbf{v}_s e^{j\theta(t)}\right\}. \tag{38a}$$

$$\because\ \mathbf{v}_s = v_e(t)\, e^{j\omega_s t + j\phi_s - j\theta(t)}$$

$$= v_e(t)\, e^{j(\omega_s t + \phi_s - \omega_0 t - \alpha\sin\omega_1 t)}. \tag{38b}$$

The state equation (37) using (38) is simulated by the Wolfram Mathematica (Ver. 14.1) [21], [22] for the parameters of Table II. As shown in Figs. 5 and 6, the transient responses of real space and the phasor space circuits are obtained assuming zero initial values. As shown in Figs. 5(a) and 6(a), the angular frequency of

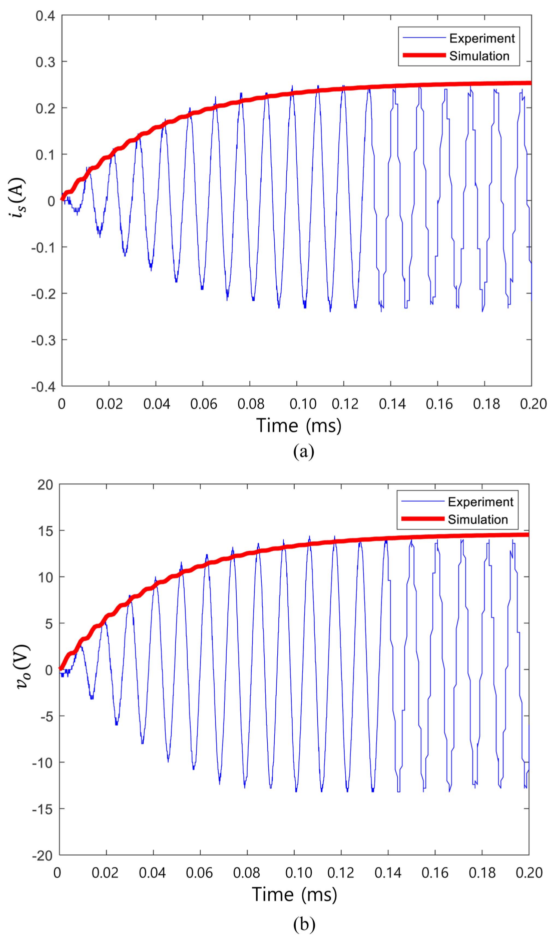

Fig. 8. Simulation and experimental waveforms for the circuit of Fig. 7. (a) $i_s(t)$. (b) $v_o(t)$at ω_s= 580 krad/s.

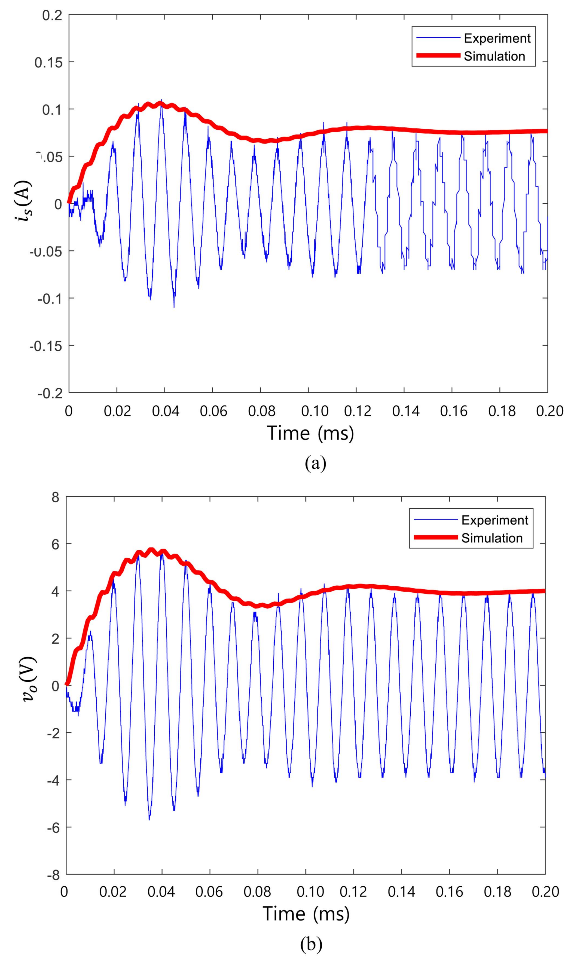

Fig. 9. Simulation and experimental waveforms for the circuit of Fig. 7. (a) $i_s(t)$.(b) $v_o(t)$at ω_s= 650 krad/s.

TABLE II
Circuit Parameters For Simulation and Experiments

Parameters	Values
ω_s	580 and 650 k rad/s
ω_0	800 k rad/s
ω_1	200 k rad/s
α	10 rad
L	100.04 µH
C	30.07 nF
R_s	3.0 Ω
R_o	2.00 kΩ

the dynamic phasor is severely time-varying and quite different from the constant source voltage angular frequency. With a step function of $v_e(t)$, $i_s$and $v_o$in real space perfectly overlap with the real part of $\mathbf{i}_s$ and $\mathbf{v}_o$ as in (1), which are shown in dotted yellow line; so, it is indistinguishable each other, as shown in the left part of Figs. 5(c) and 6(c). The phasor space variables are severely modulated and quite different from the real space ones; however, the envelopes of them, i.e., the absolute values, depict the system response, as shown in the right part of Figs. 5(c) and 6(c). The phasor space variables would simply show the envelope of real space variables if it were the conventional dynamic phasor of $\theta\ (t) = \omega_s\ t$, which is a special case of $\alpha\ =\ 0$, that becomes a generalized averaging case, as shown in Figs. 5(b) and (d) and 6(b) and (d).

Note that the envelope of the output voltage for $\theta\ (t) = \omega_s\ t$ can be analyzed from (35) for (24) and (28) [21], [22].

$$\mathbf{V}_o\ (s)\ = \mathbf{G}_v\ (s)\,\mathbf{V}_s\ (s) = \mathbf{G}_v\ (s)\,V_e\,(s)\,e^{j\phi_s} \tag{39a}$$

$$\therefore\ \mathbf{v}_o\ (t)\ = \mathcal{L}^{-1}\ \{\mathbf{V}_o\,(s)\}\ \equiv K\,\{1 - p_1\,(t)\,p_2\,(t)\} \tag{39b}$$

$$\because\ K\ = \frac{R_o e^{j\phi_s}}{R_o + R_s - LCR_o\omega_s^2 + j\omega_s\,(L + CR_oR_s)}$$

$$V_e\ (s)\ = \frac{1}{s}, p_1\ (t) = e^{-\frac{t}{2}\left(\frac{1}{CR_o} + \frac{R_s}{L}\right) - j\omega_s t}, \phi_s = 0$$

$$p_2\ (t)\ = 1 - \left\{\cos\omega_p t + \left(\frac{1}{2CR_o} + \frac{R_s}{2L} + j\omega_s\right)\frac{\sin\omega_p t}{\omega_p}\right\},$$

$$\omega_p = \frac{\sqrt{4LCR_o^2 - (L - CR_oR_s)^2}}{2LCR_o}. \tag{39c}$$

As can be seen from (39b), the beat frequency observed in the envelopes of Figs. 5(c) and 6(c) are generated from the product term of $p_1(t)p_2(t)$, where ω_s and ω_p are included in $p_1(t)$ and

$p_2(t)$, respectively. It is verified by the Mathematica simulation that (39) exactly matches the envelopes of Figs. 5(c) and 6(c).

It is identified through extensive simulation that there is no mismatch at all between the real space and phasor space circuits' waveforms for every possible change in the eight variables of Table II. Therefore, it can be said that the dynamic phasor instantly correlates the real space with the phasor space successfully, regardless of the phase angle $\theta(t)$of (2).

V. Experimental Verifications for Dynamic Phasor

The *RLC* circuit of Fig. 1 and a full bridge inverter are implemented with the parameters in Table II, as shown in Fig. 7. Note that R_s includes the overall resistance of the circuit elements, i.e., inverter internal resistance and *LC* tank resistance. The time domain phasor space response of (39b) for a step change in the envelope of the source voltage is experimentally verified at $\omega_s=$ 580 and 650 krad/s, as shown in Figs. 8 and 9, respectively. The measured waveforms of Figs. 8 and 9 are also well matched to the simulated envelopes of Figs. 5 and 6. It is observed that there is a percentage error of less than 3% in the current $i_s(t)$ and voltage $v_o(t)$ magnitudes between the simulation and experiments.

VI. Conclusion

The proposed instantaneous dynamic phasor is compared with the generalized averaging and fully verified by simulation and experiments. The dynamic phasor is instantly valid for any time and is not necessarily related to the period of the voltage or current source of ac power systems. The instantaneous dynamic phasor is valid for an arbitrary and even time-varying frequency, which is not necessarily the same as the source frequency. The transfer function of the phasor space system is found to be a frequency shift form of the original one of the real space system for the fixed frequency dynamic phasor.

Acknowledgment

The authors would like to thank Prof. Khai D. T. Ngo who reminded them of the idea of instantaneous dynamic phasor.

References

[1] C. P. Steinmetz, "Complex quantities and their use in electrical engineering," in *Proc. AIEE Int. Elect. Congr.*, 1894, pp. 33–74.

[2] N. N. Bogoliubov and Y. A. Mitropolsky, *Asymptotic Methods in the Theory of Nonlinear Oscillations*. Delhi, India: Hindustan Publishing, 1961.

[3] A. Gelb and W. E. Vander Velde, *Multiple-Input Describing Functions and Nonlinear System Design*. New York, NY, USA: McGraw-Hill, 1968.

[4] C. T. Rim and G. H. Cho, "Phasor transformation and its application to the dc/ac analyses of frequency phase-controlled series resonant converters (SRC)," *IEEE Trans. Power Electron.*, vol. 5, no. 2, pp. 201–211, Apr. 1990.

[5] S. R. Sanders, J. M. Noworolski, X. Z. Liu, and G. C. Verghese, "Generalized averaging method for power conversion circuits," *IEEE Trans. Power Electron.*, vol. 6, no. 2, pp. 251–259, Apr. 1991.

[6] C. L. DeMarco and G. C. Verghese, "Bringing phasor dynamics into the power system load flow," in *Proc. 25th North Amer. Power Symp.*, 1993, pp. 463–471.

[7] P. Mattavelli, G. C. Verghese, and A. M. Stankovic, "Phasor dynamics of thyristor-controlled series capacitor systems," *IEEE Trans. Power Syst.*, vol. 12, no. 3, pp. 1259–1267, Aug. 1997.

[8] P. Mattavelli, A. M. Stankovic, and G. C. Verghese, "SSR analysis with dynamic phasor model of thyristor-controlled series capacitor," *IEEE Trans. Power Syst.*, vol. 14, no. 1, pp. 200–208, Feb. 1999.

[9] A. M. Stanković and T. Aydin, "Analysis of asymmetrical faults in power systems using dynamic phasors," *IEEE Trans. Power Syst.*, vol. 15, no. 3, pp. 1062–1068, Aug. 2000.

[10] A. M. Stankovic, H. Lev-Ari, and M. M. Perisic, "Analysis and implementation of model-based linear estimation of dynamic phasors," *IEEE Trans. Power Syst.*, vol. 19, no. 4, pp. 1903–1910, Nov. 2004.

[11] J. A. de la O Serna, "Dynamic phasor estimates for power system oscillations," *IEEE Trans. Instrum. Meas.*, vol. 56, no. 5, pp. 1648–1657, Oct. 2007.

[12] A. Torres Muñoz and J. A. D. O. Serna, "Shanks' method for dynamic phasor estimation," *IEEE Trans. Instrum. Meas.*, vol. 57, no. 4, pp. 813–819, Apr. 2008.

[13] F. C. Jusan, S. Gomes Jr., and G. N. Taranto, "SSR results obtained with a dynamic phasor model of SVC using modal analysis," *Int. J. Elect. Power Energy Syst.*, vol. 32, no. 6, pp. 571–582, 2010.

[14] M. C. Chudasama and A. M. Kulkarni, "Dynamic phasor analysis of SSR mitigation schemes based on passive phase imbalance," *IEEE Trans. Power Syst.*, vol. 26, no. 3, pp. 1668–1676, Aug. 2011.

[15] C. T. Rim, "Unified general phasor transformation for ac converters," *IEEE Trans. Power Electron.*, vol. 26, no. 9, pp. 2465–2475, Sep. 2011.

[16] J. A. de la O Serna and J. Rodriguez-Maldonado, "Instantaneous oscillating phasor estimates with Taylor^K–Kalman filters," *IEEE Trans. Power Syst.*, vol. 26, no. 4, pp. 2336–2344, Nov. 2011.

[17] S. W. Lee, B. Choi, and Chun T. Rim, "Dynamics characterization of the inductive power transfer system for online electric vehicles by Laplace phasor transform," *IEEE Trans. Power Electron.*, vol. 28, no. 12, pp. 5902–5909, Dec. 2013.

[18] C. T. Rim, *Phasor Power Electronics*. New York, NY, USA: Springer, 2016.

[19] J. Khodaparast, "A review of dynamic phasor estimation by non-linear Kalman filters," *IEEE Access*, vol. 10, pp. 11090–11109, 2022.

[20] P. A. Ganeshamurthy, S. K. Gurumurthy, F. Ponci, and A. Monti, "A new formulation of dynamic-phasor-based state estimation with inclusion of an equality constraint," *IEEE Trans. Instrum. Meas.*, vol. 73, 2024, Art. no. 3522414.

[21] S. Wolfram, *Mathematica*, Wolfram Research, 2025. [Online]. Available: www.wolfram.com

[22] Y. Chung, *MathSymbolica*, GIST, 2025. [Online]. Available: www.mathsymbolica.com

Chun T. Rim (Fellow, IEEE) received the B.S. (Honors) degree in electrical engineering from the Kumoh National Institute of Technology, Gumi, South Korea, in 1985, and the M.S. and Ph.D. degrees in electrical engineering from the Korea Advanced Institute of Science and Technology (KAIST), Daejeon, South Korea, in 1987 and 1990, respectively.

From 2007 to 2016, he was an Associate Professor with KAIST. In 2016, he became a Full Professor with the Gwangju Institute of Science and Technology, Gwangju, South Korea. From 2018 to 2021, he was the President of Korean Energy Technology Evaluation and Planning. Since 2021, he has been the President of the Korea Energy Economics Institute, Ulsan, South Korea. He authored or coauthored 200 technical papers and wrote 19 books. He also holds 160 patents (awarded and pending). He is the author of the books *Phasor Power Electronics* (Springer, 2016) and *Wireless Power Transfer for Electric Vehicles and Mobile Devices* (Wiley, 2017).

Dr. Rim was the Co-Editor-in-Chief of IEEE Transactions on Power Electronics (TPEL). He was the recipient of numerous awards, including the Best Paper Award of IEEE TPEL in 2015 and IEEE Journal of Emerging and Selected Topics in Power Electronics in 2016, both in wireless power transfer.

Syed Ahson Ali Shah (Member, IEEE) received the B.Sc. degree in telecommunication engineering from the University of Engineering and Technology, Mardan, Pakistan, in 2015, and the M.S. and Ph.D. degrees in electronic engineering from Hanyang University, Seoul, South Korea, in 2022.

He was a Postdoctoral Researcher with Hanyang University until 2023, and since then with Gwangju Institute of Science and Technology. He authored several journal articles and conference papers. His research interests include wireless power transfer, magnetic field focusing, antennas and RF systems, implant safety, biotelemetric stents, metamaterials, 5G antennas, circuit modeling, and TMS coils.

Dr. Ahson is currently a Reviewer for Nature, Wiley, MDPI, and IEEE transactions and journals. He is an Associate Editor for *JMIR Biomedical Engineering*, an Academic Editor at Hindawi, and Guest Editor for MDPI and *PLoS One*. His Ph.D. thesis has been recognized as one of the excellent dissertations and received the Best Ph.D. Thesis Award in the overall university and the only one in the Electronic Engineering Department. He was the recipient of the IETE MN SAHA Memorial Award in 2018, the Bronze Paper Award at IEEE Student Paper Contest, Seoul, in 2019, 2021, 2022, and 2024, and the 3rd Best Student Paper Award in 2021 from the Korean Institute of Electromagnetic Engineering and Science.

Hyo J. Park received the B.S. degree in electrical engineering and computer science in 2025 from the Gwangju Institute of Science and Technology (GIST), Gwangju, South Korea, where he is currently working toward the M.S. degree in electrical engineering and computer science.

His research interests include wireless power transfer systems, inductive power transfer, magnetic field focusing, and power electronics.

Abhinandan Routray received the B.Tech. degree in electrical and electronics engineering from the Biju Patnaik University of Technology, Rourkela, India, in 2012, and the Ph.D. degree in electrical engineering from the Indian Institute of Technology (BHU), Varanasi, India, in 2021.

From 2020 to 2021, he was an Assistant Professor with the Department of Electrical and Electronics Engineering, DIT University, Dehradun, India. Then, he joined as a postdoctoral researcher with the School of Electronic and Electrical Engineering, Kyungpook National University, and, from 2021 to 2024, with the Graduate School of Electrical Convergence, Gwangju Institute of Science and Technology. He is currently an Assistant Professor with the Department of Electrical and Electronics Engineering, Manipal Institute of Technology, Manipal Academy of Higher Education, Manipal, India. He authored several research articles in IEEE/IET, Wiley journals, and high-quality IEEE/IET conference proceedings. His research interests include predictive control, wind turbine control, multilevel converters, photo voltaic (PV) inverters, modular multi-level converter (MMCs), power quality improvement, and the design of power electronics converters for microgrids and transcranial magnetic stimulation.

Dr. Routray is currently a Reviewer for IEEE TRANSACTIONS OF POWER ELECTRONICS, IEEE INDUSTRY APPLICATIONS/INFORMATICS, *IET Power Electronics*, and IEEE ACCESS.

Seog Y. Jeong (Senior Member, IEEE) received the B.S. degree in electrical engineering from Kyungpook National University, Daegu, South Korea, in 2013, and the M.S. and Ph.D. degrees in electrical engineering from the Korea Advanced Institute of Science and Technology (KAIST), Daejeon, Korea, in 2015 and 2018, respectively.

Since 2018, he has been with Samsung Electronics, where he is currently a Senior Engineer in Samsung R&D Institute. He has expertise in a wide range of element technologies such as magnetic design, power converter and circuit design, and digital controller design, including field programmable gate array (FPGA). His research interests include wide band gap (WBG) converters, energy harvesting, electromagnetic interference/electromagnetic compatibility issues, and wireless power transfer.

Dr. Jeong has been an Associate Editor for IEEE TRANSACTIONS ON POWER ELECTRONICS since 2024. He was the recipient of numerous awards, including the First Prize Paper of IEEE JOURNAL OF EMERGING AND SELECTED TOPICS IN POWER ELECTRONICS in 2016 and the Best Paper Award of 2018 IEEE WoW and 2014 IEEE EVTeC.

Youngjoo Chung (Member, IEEE) was born in Busan, South Korea, in 1959. He received the B.S. degree in physics from Seoul National University, Seoul, South Korea, in 1982, and the Ph.D. degree in plasma physics from Princeton University, Princeton, NJ, USA, in 1989.

Between 1989 and 1996, he was with the Advanced Photon Source, Argonne National Laboratory. In 1996, he returned to Korea as an Associate Professor with the Department of Information and Communications, Gwangju Institute of Science and Technology (GIST), and was promoted to Full Professor in 2001. He retired in 2025. He is currently an Emeritus Professor with GIST. His research interests include specialty optical fibers and fiber gratings, optical fiber-based devices for communication and sensing, symbolic computing, and high-performance computing.

Dr. Chung was the General Chair of the 25th International Conference on Optical Fiber Sensors (OFS-25) in 2017 and the President of the Optical Society of Korea in 2018.